WILEY

# CircATIC inhibits esophageal carcinoma progression and promotes radiosensitivity by elevating RHCG through sponging miR-10-3p

Kai Zhang[1] | Ruitai Fan[1] | Deyao Zhao[1] | Peipei Liu[2] | Zheng Yang[3] |
Junqi Liu[1] | Song Zhang[1] | Shilei Rao[3] | Yang Wang[3] | Lixin Wan[4]

[1]Department of Radiation Oncology, The First Affiliated Hospital of Zhengzhou University, Zhengzhou, Henan, China

[2]Department of Respiratory and Critical Care Medicine, Nanyang Central Hospital, Nanyang, Henan, China

[3]Department of Radiotherapy, Nanyang Central Hospital, Nanyang, Henan, China

[4]Department of Oncology, Nanyang Central Hospital, Nanyang, Henan, China

**Correspondence**

Ruitai Fan, Department of Radiation Oncology, The First Affiliated Hospital of Zhengzhou University, No. 1, Jianshe East Road, Erqi District, Zhengzhou City, Henan Province, China.
Email: fanruitai@126.com

## Abstract

**Background:** Circular RNAs (circRNAs) are implicated in the progression and radiosensitivity of human cancers, including esophageal carcinoma (ESCA). In this study, we aimed to explore the functions of circRNA 5-aminoimidazole-4-carboxamide ribonucleotide formyltransferase/IMP cyclohydrolase (circATIC) in ESCA progression.

**Methods:** CircATIC expression, miR-10b-3p and Rh family C glycoprotein (RHCG) were examined via quantitative real-time polymerase chain reaction (qRT-PCR), western blot assay or immunohistochemistry (IHC) assay. 5′-ethynyl-2′-deoxyuridine (EdU), wound-healing, transwell, and cell colony formation assays and flow cytometry analysis were conducted to evaluate cell proliferation, migration, invasion, radiosensitivity and apoptosis, respectively. Dual-luciferase reporter assay and RNA pulldown assay were conducted to analyze the relationships among circATIC, miR-10b-3p and RHCG. A murine xenograft model assay was performed to explore the functions of circATIC in tumor formation and radiosensitivity in vivo.

**Results:** CircATIC was decreased in ESCA. CircATIC overexpression suppressed cell proliferation, migration and invasion and promoted radiosensitivity and apoptosis in ESCA cells in vitro and repressed tumor formation and radioresistance in vivo. Functionally, circATIC served as the sponge for miR-10b-3p, which directly targeted RHCG. MiR-10b-3p elevation reversed circATIC-mediated effect on ESCA cell progression. Moreover, miR-10b-3p inhibition suppressed cell growth and metastasis and enhanced radiosensitivity in ESCA cells by targeting RHCG.

**Conclusions:** Overexpression of circATIC hampered ESCA progression and promoted radiosensitivity depending on the regulation of miR-10b-3p and RHCG.

**KEYWORDS**
circATIC, ESCA, miR-10b-3p, RHCG

## INTRODUCTION

Esophageal carcinoma (ESCA) is a well known common digestive tract tumor worldwide, with high incidence, rapid progression and high mortality.[1,2] The risk factors associated with ESCA include ingestion of foods containing amines, fungal infections, long-term alcohol consumption, smoking, and overheated food.[3] At present, the treatment methods for ESCA mainly include surgery, radiotherapy and chemotherapy.[4] Radiotherapy is a reasonable standard treatment option for patients with unresectable ESCA, but acquired radioresistance is a major cause of treatment failure and recurrence.[5,6] Therefore, it is necessary to explore the mechanism of radioresistance in ESCA and find possible strategies for ESCA treatment.

Circular RNAs (circRNAs) are non-coding RNAs (ncRNAs) that formed by back-splicing.[7] CircRNAs can

function as microRNA (miRNA) sponges and miRNAs can influence gene expression by combining with the 3′UTR of target mRNAs.[8,9] CircRNAs are stable than linear RNAs and play vital roles in the carcinogenesis and radiosensitivity of human cancers.[10] For example, Yue et al. declared that circ_0006948 contributed to the malignancy of ESCA.[11] Circ-ABCB10 aggravated the growth and invasion of esophageal squamous cell carcinoma (ESCC) through miR-670-3p.[12] Circ_0000554 inhibited the radiosensitivity in ESCA by adsorbing miR-485-5p and upregulating FERMT1.[13] These reports demonstrated the involvement of circRNAs in ESCA progression and radiosensitivity. CircRNA 5-aminoimidazole-4-carboxamide ribonucleotide formyltransferase/IMP cyclohydrolase (circATIC; also named as hsa_circ_0058058 and hsa_circ_102913) was downregulated in radioresistant ESCA cells.[14] However, it is still unclear whether circATIC plays a role in the radiosensitivity in ESCA.

Accumulating evidence has verified the pivotal roles of miRNAs in tumor progression and radioresistance.[15,16] In ESCA, diverse miRNAs, such as miR-199a-3p,[17] miR-338-5p,[18] miR-124[19] and miR-96,[20] have been identified to be related to tumorigenesis and radiosensitivity. As for miR-10b-3p, previous studies have demonstrated its promotional effect on ESCA development.[21,22] However, the relationship between miR-10b-3p and radioresistance in ESCA has not yet been reported.

In this study, bioinformatic analysis showed that miR-10b-3p contained the binding sites of circATIC and Rh family C glycoprotein (RHCG). We aimed to elucidate the roles and relationships of circATIC, miR-10b-3p and RHCG in the regulation of ESCA development and radiosensitivity.

## METHODS

### Tissue collection

A total of 64 ESCA patients at Nanyang Central Hospital were recruited into this study. After the Ethics Committee of Nanyang Central Hospital approved this study and all patients signed written informed consents, the tumor tissues and adjacent normal tissues were harvested from the patients. The patients were grouped into tumor node metastasis (TNM) stage I + II ($N = 40$) and TNM stage III ($N = 24$), as well as divided into negative ($N = 42$) and positive ($N = 22$) lymph node metastasis groups. The tissues were stored at $-80°C$ until use.

### Cell culture

Human normal esophageal epithelial cell line (HET-1A) and ESCC cell lines (KYSE150 and EC109) were all offered by BeNa Culture Collection. All cells were kept in DMEM (Invitrogen) supplemented with 10% fetal bovine serum (FBS; Invitrogen) and 1% penicillin/streptomycin (Invitrogen) in the conditions of 37°C and 5% $CO_2$.

**TABLE 1** Primers sequences used for qRT-PCR

| Name | | Primers for PCR (5′-3′) |
| --- | --- | --- |
| circATIC (hsa_circ_0058058) | Forward | CCAGTTAGCCTTGAAGCCTTA |
| | Reverse | GCAAAGTTTTCACACGTCCC |
| RHCG | Forward | GGTTCCACTTCTTACAAGACCG |
| | Reverse | GGGCTGACTTTACCCAGAACT |
| miR-10b-3p | Forward | GGATTCCGAGTACAGTATAGATGA |
| | Reverse | TCAACTGGTGTCGTGGAGT |
| β-actin | Forward | CTTCGCGGGCGACGAT |
| | Reverse | CCACATAGGAATCCTTCTGACC |
| U6 | Forward | CTTCGGCAGCACATATACT |
| | Reverse | AAAATATGGAACGCTTCACG |

## Quantitative real-time polymerase chain reaction (qRT-PCR) assay

Total RNA was isolated with TRIzol (Invitrogen) and reversely transcribed into cDNAs using PrimeScript first strand cDNA synthesis reagent (Takara) or MiX-x miRNA synthesis reagent (TaKaRa). Next, SYBR Premix DimerEraser (Takara) was employed for qRT-PCR. The Ct value was normalized to β-actin or U6 through $2^{-\Delta\Delta Ct}$ way. The primers were shown in Table 1.

## Subcellular fractionation location assay

By utilizing the cytoplasmic and nuclear RNA purification kit (Norgen Biotek), the nucleus and cytoplasm were isolated from EC109 and KYSE150 cells referring to the protocols. The expression of circATIC in the nucleus and cytoplasm was detected.

## RNase R treatment

To estimate the ring feature of circATIC, total RNA in EC109 and KYSE150 cells was treated with or without RNase R (Geneseed). CircATIC and β-actin expression was examined.

## Cell transfection

CircATIC overexpression vector (circATIC) and its control (vector), miR-10b-3p mimic (miR-10b-3p) and its control (miR-NC), miR-10b-3p inhibitors (anti-miR-10b-3p) and its control (anti-NC), siRNA against RHCG (si-RHCG) and scramble control (si-NC) were all synthesized by

GenePharma. Then the transfections were done via Lipofectamine 3000 (Invitrogen).

## 5′-ethynyl-2′-deoxyuridine (EdU) assay

EdU assay reagent (Ribibio) was adopted to assess cell proliferation ability. In brief, the transfected cells in 24-well plates were treated with EdU for 12 h, immobilized with 4% paraformaldehyde (Sigma-Aldrich) and permeabilized with 0.5% Triton-X-100 (Sigma-Aldrich). Subsequently, the nuclei were dyed with EdU and DAPI. The EdU-positive cells were assessed under a fluorescence microscope (Olympus).

## Wound-healing assay

After the transfected cells were seeded into 6-well plates and maintained until 100% confluence, a pipette tip was utilized to make wounds on the plates. The width of the scratch was measured at 0 and 24 h to estimate the migration ability.

## Transwell assay

The transwell chambers (Corning) with Matrigel (Corning) coverage were used to evaluate cell invasion. In short, the transfected EC109 and KYSE150 cells were suspended in serum-free medium and then added into the upper chamber. The complete medium was added into the lower chamber. 24 h later, cells invaded into the lower chamber were dyed with crystal violet (Sigma-Aldrich). The invaded cells were visualized and quantified under a microscope (100×; Olympus).

## Colony formation assay

The transfected EC109 and KYSE150 cells were irradiated with X-ray at different radiation doses and then seeded into 6-well plates. After cultivation for 14 days, the colonies were dyed with crystal violet (Sigma-Aldrich). The survival fraction was analyzed to evaluate cell radiosensitivity.

## Flow cytometry analysis

The Annexin V-fluorescein isothiocyanate (FITC)/propidium iodide (PI) apoptosis detection kit (Beyotime) was used to analyze cell apoptosis. EC109 and KYSE150 cells with various transfection were plated into 12-well plates and exposed to radiation (4 Gy). Next, the cells were suspended in binding buffer and dyed with Annexin V-FITC and PI for 15 min. The apoptotic cells were estimated via flow cytometry (BD Biosciences).

## Western blot assay

Total protein was isolated using RIPA lysis buffer (Beyotime) and quantified using BCA protein assay reagent (Beyotime). After being separated through SDS-PAGE electrophoresis, the proteins were transferred onto PVDF membranes. Next, the membranes were blocked in 5% skimmed milk, incubated overnight with primary antibodies against bcl-2 (ab196495; Abcam), bax (ab104156; Abcam), c-caspase3 (ab32042; Abcam), RHCG (ab187904; Abcam) and β-actin (ab8224; Abcam), and then incubated with secondary antibody (ab2302; Abcam) for 1 h. The ECL kit (Beyotime) was used to visualize the protein bands.

## Dual-luciferase reporter assay

The fragments of circATIC or RHCG 3′UTR including the wild-type (WT) or corresponding mutant (MUT) binding sites of miR-10b-3p were cloned and injected into pmirGLO (Promega) to construct the dual-luciferase reporter vectors. Next, the vectors were introduced into EC109 and KYSE150 cells together with miR-NC/miR-10b-3p. The luciferase intensity was examined with dual-luciferase reporter assay reagent (Promega).

## RNA pulldown assay

The wild-type or mutated miR-10b-3p biotin-labeled probe (miR-10b-3p-WT and miR-10b-3p-MUT) was offered by Ribobio and introduced into EC109 and KYSE150 cells. The cells were then cultured with the streptavidin-coated magnetic beads (Invitrogen) to generate probe-coated beads. The enrichment of circATIC in the biotin-coupled RNA complexes was determined.

## Murine xenograft model

The EC109 cells with vector or circATIC transfection were injected into the BALB/c nude mice (Beijing Vital River Laboratory Animal Technology Co., Ltd.) and then the mice in vector ($N = 10$) and circATIC ($N = 10$) groups were divided into the irradiation group (vector+4 Gy and circATIC+4 Gy; $N = 5$/group) and the nonirradiation group (vector and circATIC; $N = 5$/group). Seven days later, the mice in the irradiation group were treated with x-xays (4 Gy) every three days. The tumor volume (volume = $0.5 \times$ length $\times$ width$^2$) was estimated every seven days. The mice were killed after 28 days and tumors were weighed. This in vivo experiment was permitted by the Ethics Committee of Animal Research of Nanyang Central Hospital.

## Immunohistochemistry (IHC) assay

IHC assay was performed to examine the expression of Ki67, RHCG and c-caspase3 in the xenograft tumors as previously described.[23] The antibodies against Ki67 (ab15580), RHCG (ab187904) and c-caspase3 (ab32042) were provided by Abcam.

## Statistical analysis

The experiments were conducted in triplicate and analyzed utilizing GraphPad Prism 7. The results are shown as mean $\pm$ SD. Student's $t$-test or one-way ANOVA was utilized for different analyses. $p < 0.05$ was considered statistically significant.

## RESULTS

### Low expression of circATIC in ESCA tissues and cells

Originally, circATIC expression in ESCA tissues and adjacent normal tissues was detected by qRT-PCR. The results showed that circATIC was weakly expressed in tumor tissues compared to normal tissues (Figure 1a). CircATIC was downregulated in higher TNM stage (TNM III; $N = 24$) and positive lymph node metastasis ($N = 22$) groups compared to lower TNM stages (I + II; $N = 40$) and lymph node metastasis ($N = 42$) groups (Figure 1b,c). Compared to HET-1A cells, circATIC level was decreased in KYSE150 and EC109 cells (Figure 1d). CircATIC was also named as hsa_circ_0058058 and derived from the exons 2–6 of ATIC (Figure 1e). Subcellular fractionation location assay showed that circATIC was mainly enriched in the cytoplasm of EC109 and KYSE150 cells (Figure 1f,g). RNase R assay showed that circATIC was resistant to RNase R treatment, indicating the circular feature of circATIC (Figure 1h,i). These findings indicated that the dysregulation of circATIC might be involved in ESCA progression.

### Overexpression of circATIC suppressed cell proliferation, migration and invasion and promoted radiosensitivity in ESCA cells

To explore the functions of circATIC in ESCA progression, oe-circATIC was transfected into EC109 and KYSE150 cells to enhance circATIC expression, which was verified by qRT-PCR assay (Figure 2a). EdU assay showed that circATIC overexpression suppressed the proliferation of EC109 and KYSE150 cells compared to vector control groups (Figure 2b). Wound-healing assay indicated that circATIC enhancement suppressed the capacity of EC109 and KYSE150 cells to migrate in comparison with control groups (Figure 2c). As illustrated by transwell assay, circATIC

overexpression repressed the invasion of EC109 and KYSE150 cells in comparison with vector control groups (Figure 2d). Moreover, the cell survival fraction of EC109 and KYSE150 cells transfected with oe-circATIC was reduced under different doses of radiation, suggesting that circATIC overexpression enhanced cell radiosensitivity (Figure 2e,f). Flow cytometry analysis indicated that radiation exposure facilitated the apoptosis of EC109 and KYSE150 cells, moreover, circATIC overexpression further increased cell apoptosis under radiation exposure (Figure 2g). In addition, the protein level of bcl-2 was reduced and the protein levels of bax and c-caspase3 in EC109 and KYSE150 cells were increased after radiation exposure, while circATIC further enhanced the effects of radiation exposure on bcl-2, bax and c-caspase3 levels (Figure 2h,i). In addition, the effect of circATIC knockdown on the radiosensitivity was investigated. As shown in Figure S1a, si-circATIC transfection led to a marked reduction in circATIC expression in EC109 and KYSE150 cells compared to the si-NC control group. CircATIC knockdown reduced cell radiosensitivity (Figure S1b,c). Flow cytometry analysis showed that radiation exposure promoted EC109 and KYSE150 cell apoptosis, while circATIC knockdown rescued the effect (Figure S1d). In addition, bcl-2 level was reduced and bax and c-caspase3 levels were elevated in EC109 and KYSE150 cells, while circATIC silencing reversed the effects (Figure S1e,f). All these findings suggested that circATIC overexpression restrained ESCA cell growth and metastasis and promoted radiosensitivity.

### CircATIC functioned as a sponge for miR-10b-3p

Through analyzing circbank (http://www.circbank.cn/), miR-10b-3p was found to be a target of circATIC. TCGA analysis showed that miR-10b-3p was upregulated in ESCA tissues compared to normal controls (Figure 3a). We then detected miR-10b-3p expression in 64 ESCA tissues and found that miR-10b-3p was highly expressed in ESCA tissues compared to normal tissues (Figure 3b). High expression of miR-10b-3p was related to advanced TNM stage and positive lymph node metastasis (Figure 3c,d). Moreover, miR-10b-3p level was markedly increased in KYSE150 and EC109 cells compared to HET-1A cells (Figure 3e). The complementary sequences between circATIC and miR-10b-3p were shown in Figure 3f. MiR-10b-3p mimic transfection markedly increased miR-10b-3p expression in EC109 and KYSE150 cells relative to miR-NC transfected cells (Figure 3g). To further estimate the relationship between miR-10b-3p and circATIC, dual-luciferase reporter assay and RNA pulldown assay were conducted. As demonstrated by dual-luciferase reporter assay, miR-10b-3p overexpression reduced the luciferase activity of circATIC-WT, but did not affect the luciferase activity of circATIC-MUT in EC109 and KYSE150 cells (Figure 3h,i). RNA pulldown assay showed that miR-10b-3p-WT could pulldown more
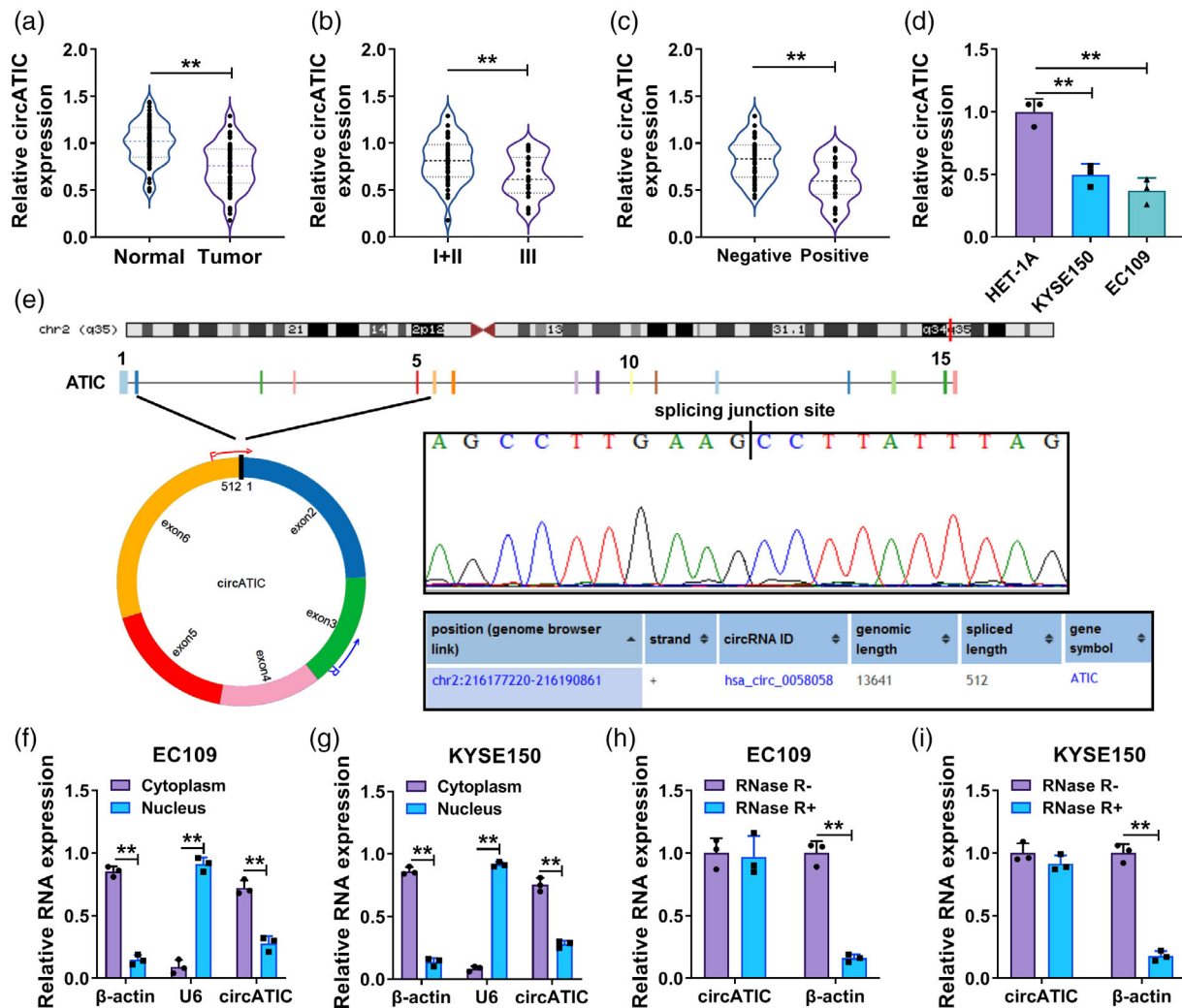
**FIGURE 1** CircATIC was downregulated in ESCA tissues and cells. (a) CircATIC expression in ESCA tissues and normal tissues was detected by qRT-PCR assay. (b) CircATIC expression in ESCA tissues at different TNM stages was detected by qRT-PCR. (c) CircATIC expression in tumor tissues with positive or negative lymph node metastasis was detected by qRT-PCR. (d) CircATIC expression in HET-1A, KYSE150 and EC109 was examined by qRT-PCR. (e) CircATIC was derived from ATIC gene. (f and g) CircATIC expression in the cytoplasm and nucleus of EC109 and KYSE150 cells was quantified by qRT-PCR. (h and i) After RNase R treatment, circATIC expression in EC109 and KYSE150 cells was detected by qRT-PCR. **$p < 0.01$

circATIC than miR-NC or miR-10b-3p-MUT (Figure 3j). These results indicated that circATIC directly bound to miR-10b-3p.

## CircATIC overexpression inhibited the malignancy behaviors and promoted radiosensitivity in ESCA cells by targeting miR-10b-3p

To explore the relationship between circATIC and miR-10b-3p in regulating ESCA progression, EC109 and KYSE150 cells were transfected with vector+miR-NC, oe-circATIC+miR-NC or oe-circATIC+miR-10b-3p. As illustrated by EdU assay, circATIC overexpression hampered the proliferation of EC109 and KYSE150 cells, while miR-10b-3p mimic transfection reversed the effect (Figure 4a). Wound healing

and transwell assays showed that oe-circATIC-mediated suppressive roles in EC109 and KYSE150 cell migration and invasion were abated by increasing miR-10b-3p (Figure 4b,c). Cell colony formation assay showed that circATIC enhancement promoted radiosensitivity in EC109 and KYSE150 cells, but miR-10b-3p reversed the impact (Figure 4d,e). Flow cytometry analysis indicated that circATIC overexpression induced the apoptosis of EC109 and KYSE150 cells under radiation exposure, whereas the effect was rescued by upregulating miR-10b-3p (Figure 4f). The effects of circATIC overexpression on bcl-2, bax and c-caspase3 protein levels in EC109 and KYSE150 cells with radiation exposure were also ameliorated by miR-10b-3p elevation (Figure 4g,h). Collectively, circATIC overexpression repressed cell proliferation, motility and radioresistance in ESCA cells by targeting miR-10b-3p.
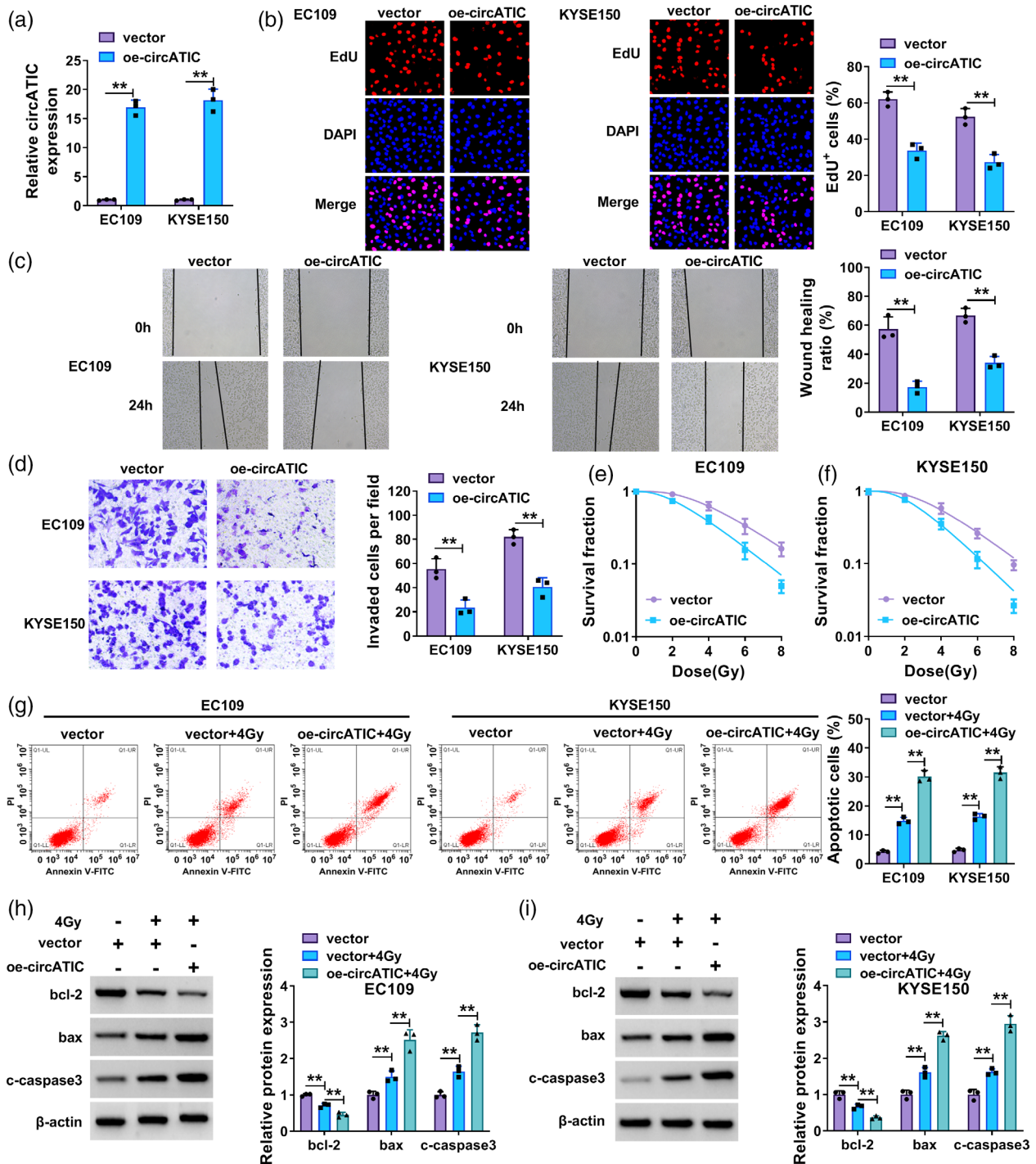
**FIGURE 2** Effects of circATIC on ESCA cell proliferation, migration, invasion and radiation. EC109 and KYSE150 cells were transfected with vector or oe-circATIC. (a) CircATIC expression in EC109 and KYSE150 cells was detected by qRT-PCR. (b–d) The proliferation, migration and invasion of EC109 and KYSE150 cells were evaluated by EdU assay, wound-healing assay and transwell assay, respectively. (e and f) The survival fraction of EC109 and KYSE150 cells under different doses of radiation (2, 4, 6 and 8 Gy) was analyzed by colony formation assay. (g) The apoptosis of transduced EC109 and KYSE150 cells upon radiation was analyzed by flow cytometry analysis. (h and i) The protein levels of bcl-2, bax and c-caspase3 in the transfected EC109 and KYSE150 cells under radiation exposure were measured via western blot assay. **$p < 0.01$

## RHCG was the target gene of miR-10b-3p

A Venn diagram showed that 11 genes were simultaneously predicted to the target gene of miR-10b-3p through Targetscan (http://www.targetscan.org/vert_71/?tdsourcetag=

s_pcqq_aiomsg) and GEPIA (http://gepia.cancer-pku.cn/detail.php) (Figure 5a). RHCG was then selected as our study object. Moreover, GEPIA database showed that RHCG was downregulated in ESCA tissues compared to normal tissues (Figure 5b). Compared to normal tissues, RHCG mRNA
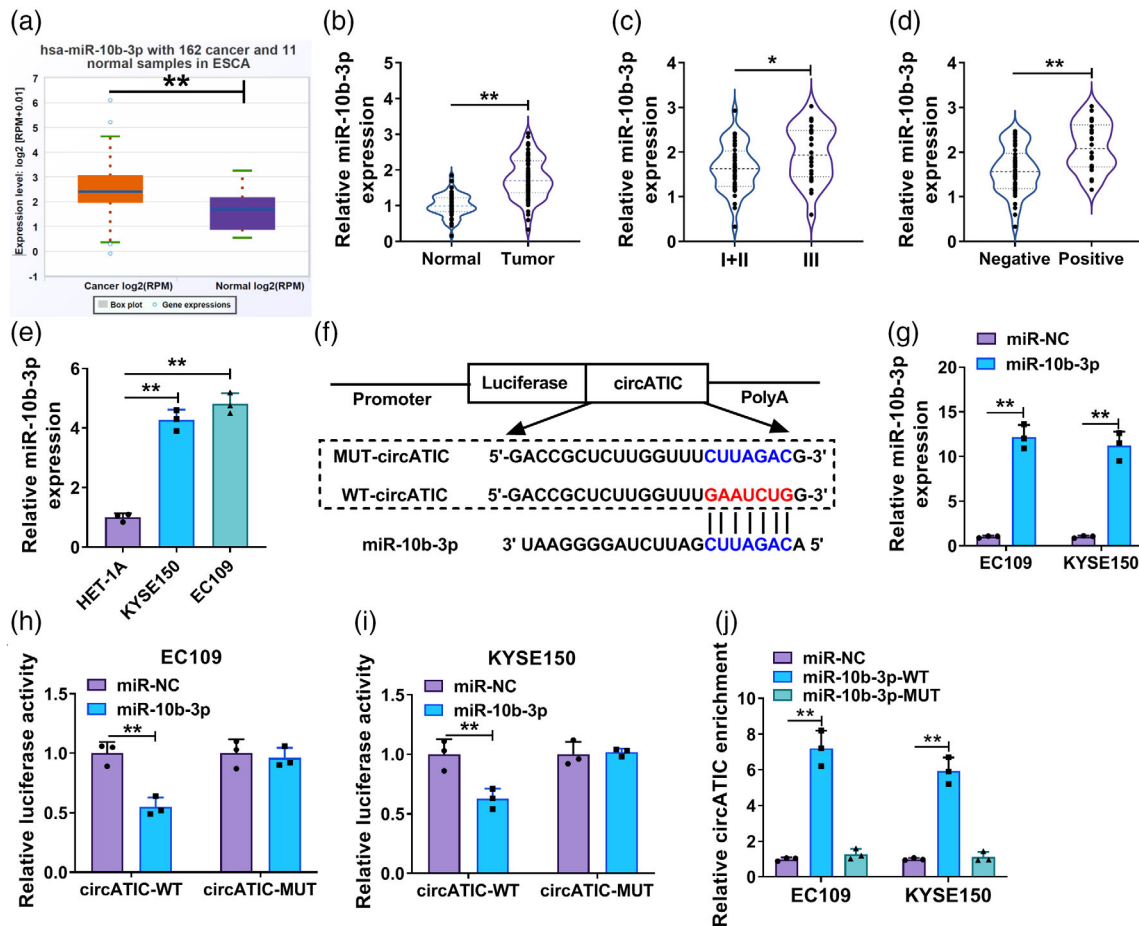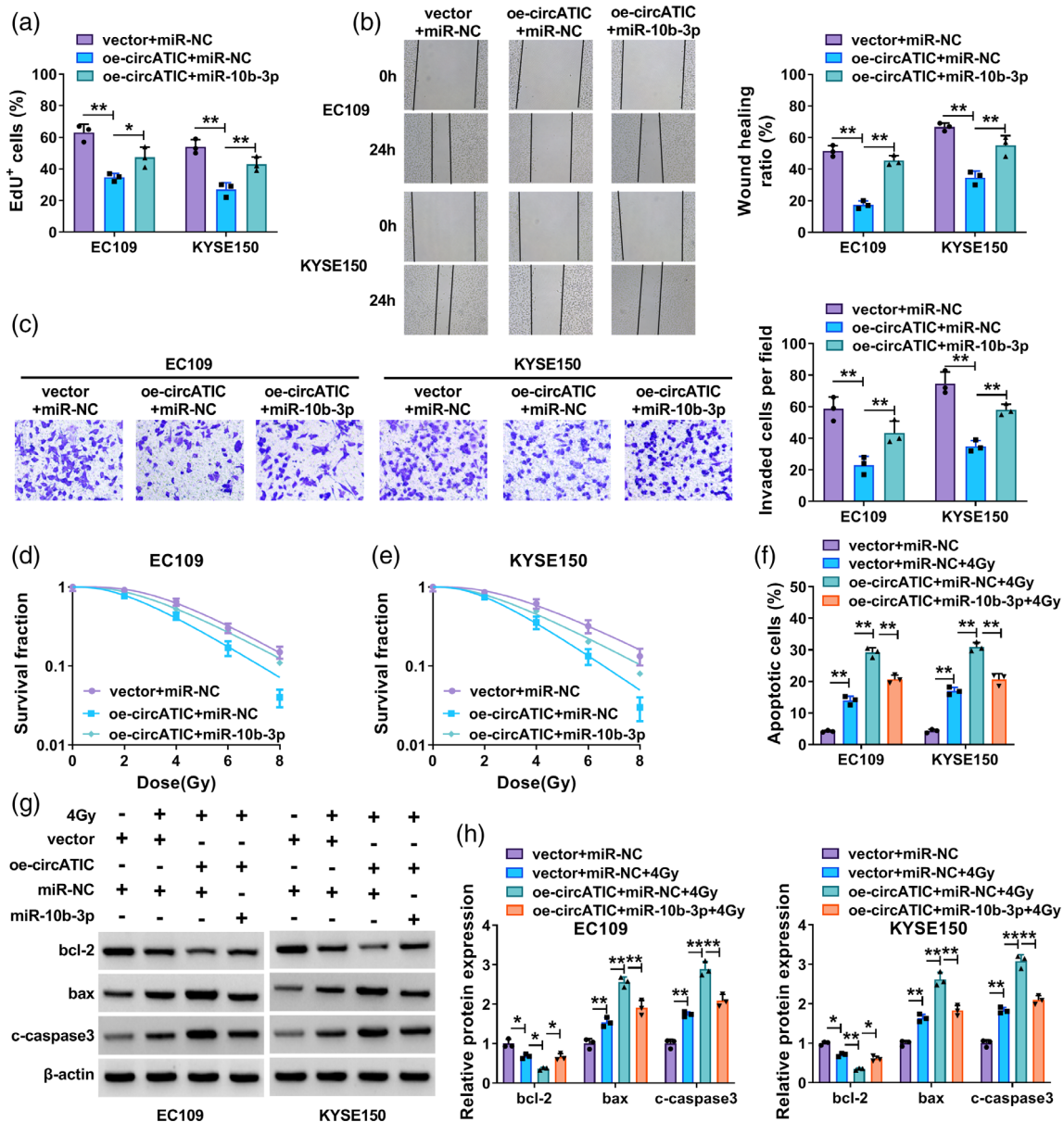
**FIGURE 3** CircATIC directly targeted miR-10b-3p. (a) TCGA database showed miR-10b-3p expression was increased in ESCA. (b) MiR-10b-3p expression in ESCA tissues and normal tissues was detected by qRT-PCR. (c) MiR-10b-3p expression in the tumors at different TNM stages was measured by qRT-PCR. (d) MiR-10b-3p expression in the tumors with positive or negative lymph node metastasis was measured by qRT-PCR. (e) MiR-10b-3p expression in HET-1A, KYSE150 and EC109 cells was determined by qRT-PCR. (f) The binding sites between circATIC and miR-10b-3p. (g) MiR-10b-3p expression in EC109 and KYSE150 cells transfected with miR-NC or miR-10b-3p was detected by qRT-PCR. (h–j) The relationship between circATIC and miR-10b-3p was demonstrated through dual-luciferase reporter assay and RNA pull down assay. $*p < 0.05$, $**p < 0.01$

level was decreased in tumor tissues ($N = 64$) (Figure 5c). Low expression of RHCG was found in ESCA patients with advanced TNM stages and negative lymph node metastasis (Figure 5d,e). Moreover, RHCG protein level was evidently decreased in ESCA tissues and cells in comparison with normal tissues and cells (Figure 5f,g). There were two complementary sequences between miR-10b-3p and RHCG at positions 771–777 and 2705–2712 of RHCG 3'UTR (Figure 5h). Overexpression of miR-10b-3p drastically inhibited the luciferase activity of WT-RHCG-3'UTR at different positions in both EC109 and KYSE150 cells, but the luciferase activity of MUT-RHCG-3'UTR was not changed (Figure 5i–l). The results further verified the combination between miR-10b-3p and RHCG. In addition, our results exhibited that miR-10b-3p overexpression led to a reduction in RHCG protein level in EC109 and KYSE150 cells compared to miR-NC control group (Figure 5m). Taken together, miR-10b-3p regulated RHCG expression by targeting RHCG.

## MiR-10b-3p inhibition suppressed cell proliferation, migration, invasion and radioresistance by targeting RHCG

As shown in Figure 6a, si-RHCG transfection markedly suppressed RHCG protein level in EC109 and KYSE150 cells compared to si-NC control groups. The transfection of anti-miR-10b-3p distinctly decreased miR-10b-3p expression in EC109 and KYSE150 cells relative to anti-NC groups (Figure 6b). Next, the relationship between miR-10b-3p and RHCG in regulating ESCA progression was explored. As illustrated by EdU assay, wound-healing assay and transwell assay, miR-10b-3p inhibition repressed the proliferation, migration and invasion of EC109 and KYSE150 cells, while these effects were weakened by silencing RHCG (Figure 6c–e). The results of colony formation assay showed that miR-10b-3p inhibition suppressed the survival fraction of EC109 and KYSE150 cells under radiation exposure, while RHCG deficiency partially abrogated the effect (Figure 6f,g).

**FIGURE 4** CircATIC directly targeted miR-10b-3p to regulate ESCA cell growth, metastasis and radiosensitivity. EC109 and KYSE150 cells were transfected with vector+miR-NC, oe-circATIC+miR-NC or oe-circATIC+miR-10b-3p. (a–c) The proliferation, migration and invasion of EC109 and KYSE150 cells were assessed by EdU, wound-healing and transwell assays, respectively. (d and e) Under different doses of radiation, cell survival was analyzed by colony formation assay. (f) The apoptosis of EC109 and KYSE150 cells under radiation was estimated by flow cytometry analysis. (g and h) The protein levels of bcl-2, bax and c-caspase3 in EC109 and KYSE150 cells upon radiation were measured through western blot assay. *$p < 0.05$, **$p < 0.01$

Flow cytometry analysis indicated that the apoptosis of EC109 and KYSE150 cells was promoted by miR-10b-3p inhibition under radiation exposure, with RHCG silencing rescued the effect (Figure 6h). Furthermore, miR-10b-3p inhibition reduced bcl-2 level and elevated bax and c-caspase3 levels in EC109 and KYSE150 cells upon radiation, but RHCG knockdown abated the effects (Figure 6i,j). All these results suggested that miR-10b-3p inhibition suppressed cell malignant behaviors and promoted radiosensitivity in ESCA cells through regulating RHCG.

## CircATIC/miR-10b-3p/RHCG axis regulated cell proliferation, migration, invasion and radiosensitivity in ESCA cells

As shown in Figure 7a, circATIC overexpression promoted RHCG protein level in EC109 and KYSE150 cells, while the effect was rescued by increasing miR-10b-3p. A schematic diagram shows that circATIC knockdown promoted proliferation, migration and invasion and suppressed radiosensitivity in ESCA cells by miR-10b-3p/RHCG pathway (Figure 7b).
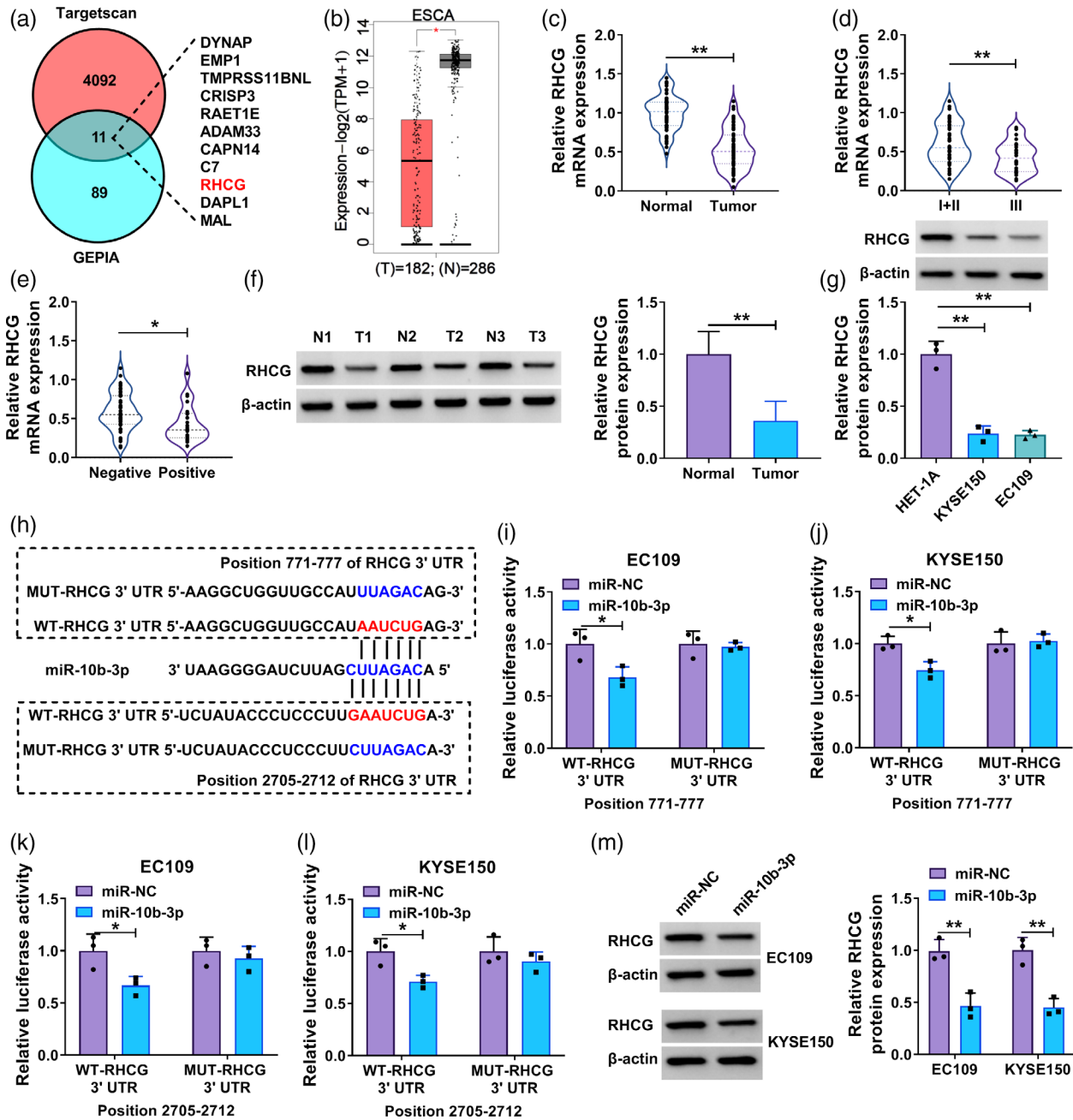
**FIGURE 5** RHCG was targeted by miR-10b-3p. (a) The target genes of miR-10b-3p were predicted by Targetscan and GEPIA. (b) Low expression of RHCG in ESCA. (c) The mRNA level of RHCG in ESCA tissues and normal tissues was detected by qRT-PCR. (d and e) The mRNA level of RHCG in ESCA patients with different TNM stages, positive and negative lymph node metastasis was detected by qRT-PCR. (f and g) The protein level of RHCG in tumor tissues and cells was measured via western blot assay. (h) The binding sites between RNCG and miR-10b-3p. (i–l) The interaction between miR-10b-3p and RHCG was demonstrated by dual-luciferase reporter assay. (m) The protein level of RHCG in EC109 and KYSE150 cells transfected with miR-NC or miR-10b-3p was measured by western blot assay. $*p < 0.05$, $**p < 0.01$

## CircATIC overexpression suppressed tumor growth and promoted radiosensitivity in vivo

Finally, the functions of circATIC in tumor growth and radiosensitivity in ESCA, in vivo experiments were further performed. As shown in Figure 8a, radiation exposure and circATIC overexpression did not affect the bodyweight of the mice. Radiation exposure or circATIC overexpression markedly inhibited tumor volume and tumor weight, moreover, circATIC overexpression enhanced the inhibitory effects of radiation on tumor volume and weight (Figure 8b,c). Additionally, Ki67 and RHCG levels were decreased and c-caspase3 level was increased in the xenograft tumors in circATIC and
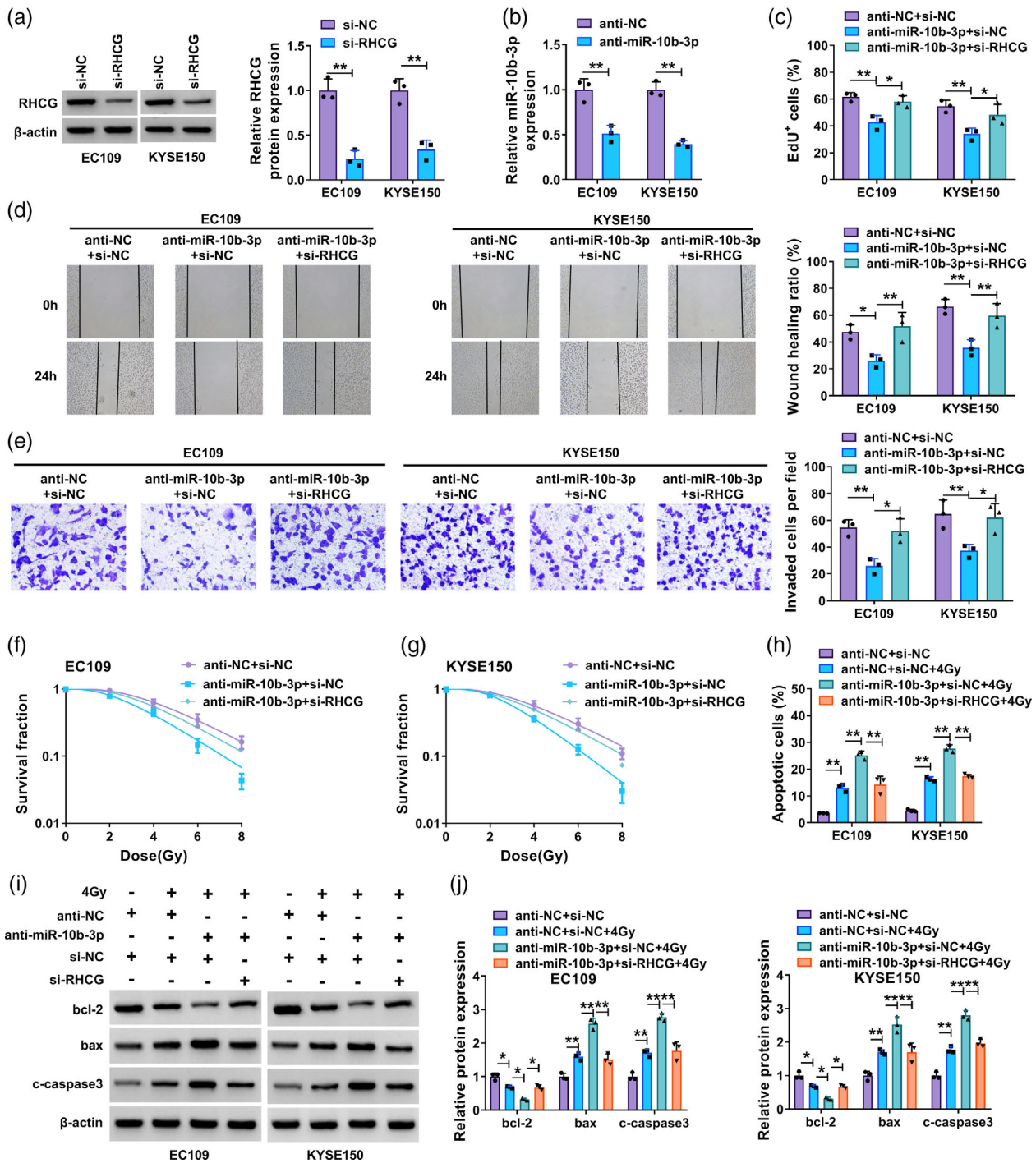
**FIGURE 6** MiR-10b-3p inhibition suppressed cell growth and motility and enhanced radiosensitivity in ESCA cells by targeting RHCG. (a) The protein level of RHCG in EC109 and KYSE150 cells transfected with si-NC or si-RHCG was measured by western blot assay. (b) MiR-10b-3p expression in EC109 and KYSE150 cells with anti-NC or anti-miR-10b-3p transfected was detected by qRT-PCR. (c–j) EC109 and KYSE150 cells were transfected with anti-NC +si-NC, anti-miR-10b-3p+si-NC or anti-miR-10b-3p+si-RHCG. (c–g) The proliferation, migration, invasion and survival fraction of EC109 and KYSE150 cells were estimated by EdU, wound-healing, transwell and colony formation assays, respectively. (h) The apoptosis of EC109 and KYSE150 cells under radiation exposure was analyzed by flow cytometry analysis. (i and j) The protein levels of bcl-2, bax and c-caspase3 in EC109 and KYSE150 cells upon radiation were examined via western blot assay. *$p < 0.05$, **$p < 0.01$

circATIC+4Gy groups compared to vector and vector +4Gy groups (Figure 8d). Taken together, circATIC repressed tumors growth and facilitated radiosensitivity in vivo.

## DISCUSSION

Radioresistance is a vital reason for the failure of cancer treatment.[6] Thus, discovering methods to relieve
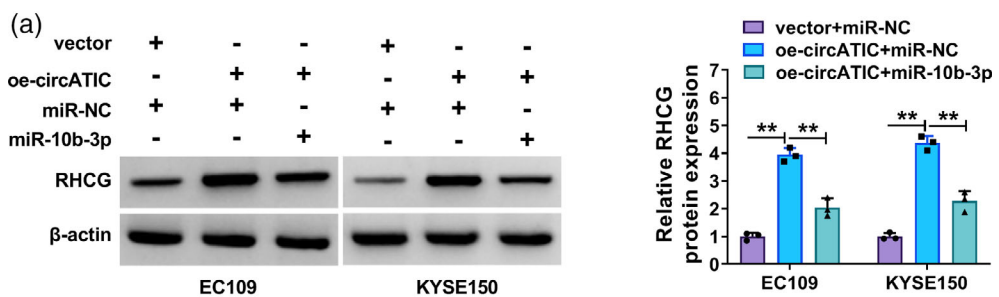
**FIGURE 7** CircATIC/miR-10b-3p/RHCG affected ESCA cell progression. (a) The protein level of RHCG in EC109 and KYSE150 cells transfected with vector+miR-NC, oe-circATIC+miR-NC or oe-circATIC+miR-10b-3p was determined by western blot assay. (b) A schematic diagram of circATIC in regulating ESCA progression. **$p < 0.01$
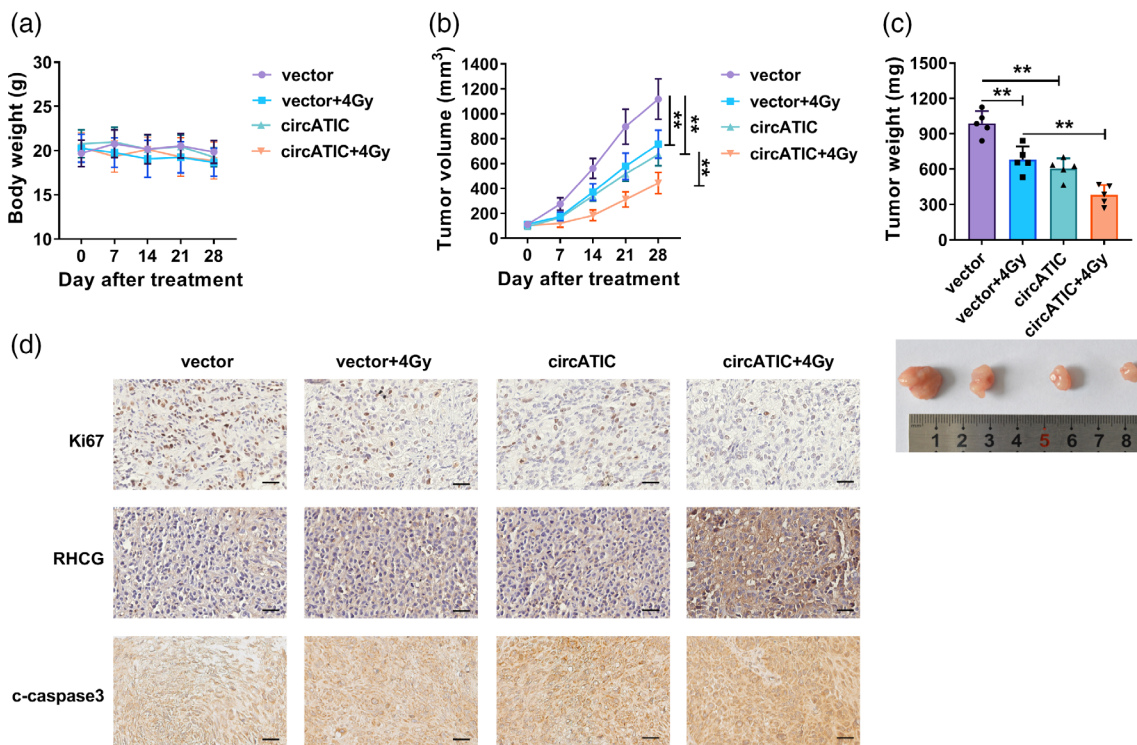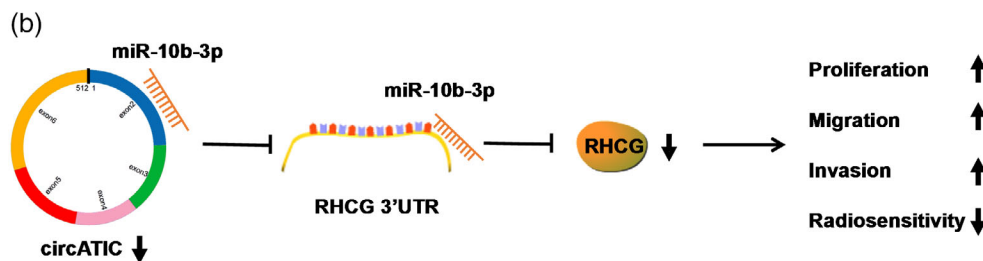


**FIGURE 8** CircATIC overexpression inhibited tumorigenesis and promoted radiosensitivity in vivo. (a) The bodyweight in different groups was examined. (b and c) Tumor volume and weight were measured. (d) The expression of Ki67, RHCG and c-caspase3 in xenograft tumors was examined. **$p < 0.01$

radioresistance is helpful for cancer therapy. CircRNAs are involved in the radioresistance of cancers.[24] In this study, the promotional effect of circATIC on radiosensitivity was explored. Moreover, the potential mechanism of circATIC was identified.

In ESCA, the involvement of circRNAs in tumor progression and radiosensitivity has been reported. For example, circ_0000554 accelerated cell growth and motility and repressed radiosensitivity in ESCA by upregulating FERMT1 through sponging miR-485-5p.[13] Circ-PRMT5 aggravated the migration of ESCA by interacting with miR-203.[25] Circ_0003340 triggered the invasion and growth of ESCA via miR-564/TPX2.[26] Even so, multiple circRNAs in ESCA have not been elucidated. CircATIC (hsa_circ_0058058) was reported to repress the progression of acute myeloid leukemia and multiple myeloma by regulating miR-4319/EIF5A2

axis or miR-338-3p/ATG14 axis.[27,28] In this study, circATIC was found to be lowly expressed in ESCA and low expression of circATIC was related to advanced TNM stage and positive lymph node metastasis. These outcomes indicated that circATIC might be a diagnostic marker in ESCA. Then we further investigated the functions of circATIC in ESCA. It was found that circATIC overexpression restrained the growth, metastasis and radioresistance and induced apoptosis in ESCA cells. Moreover, in vivo experiments demonstrated that circATIC repressed tumor formation and enhanced radiosensitivity in vivo.

Subsequently, the underlying mechanism of circATIC was investigated. It was discovered that miR-10b-3p was the target of circATIC for the first time. Zhang et al. and Lu et al. disclosed that miR-10b-3p elevation caused the promotion on cell growth, migration and invasion as well as the inhibition on apoptosis in ESCA.[21,22] In line with the reports, miR-10b-3p was increased in ESCA and miR-10b-3p inhibition hampered the malignant phenotypes of ESCA cells. In addition, the impact of miR-10b-3p on the radiosensitivity in ESCA was first clarified. As a result, miR-10b-3p downregulation enhanced the sensitivity of ESCA cells to radiation. Of note, circATIC overexpression-mediated impacts on ESCA cell progression and radiosensitivity were abated by increasing miR-10b-3p, suggesting that circATIC modulated ESCA development and radioresistance by adsorbing miR-10b-3p.

RHCG belongs to the Rhesus (Rh) family and is widely expressed in different tissues requiring ammonia metabolism for normal biological functions such as kidney, liver, central nervous system and gastrointestinal tract.[29,30] Moreover, Ming et al. declared that RHCG was reduced in ESCC and repressed the growth and motility of ESCC.[31] Herein, RHCG was verified to be the target of miR-10b-3p and was decreased in ESCA. Furthermore, miR-10b-3p could target RHCG to inhibit cell malignant behaviors and radioresistance in ESCA cells.

In conclusion, the relationships among circATIC, miR-10b-3p and RHCG were first identified. CircATIC decelerated the progression and promoted radiosensitivity of ESCA by modulating miR-10b-3p/RHCG axis. This study might offer a potential marker for ESCA diagnosis and radiotherapy.

## ACKNOWLEDGMENTS

## CONFLICT OF INTEREST
The authors declare that they have no conflicts of interest.

## ORCID
Kai Zhang 🄳 https://orcid.org/0000-0002-0087-9081
Ruitai Fan 🄳 https://orcid.org/0000-0002-1371-8930

## REFERENCES
1. Chen W, Zheng R, Baade PD, Zhang S, Zeng H, Bray F, et al. Cancer statistics in China, 2015. CA Cancer J Clin. 2016;66(2):115–32.

2. Huang FL, Yu SJ. Esophageal cancer: risk factors, genetic association, and treatment. Asian J Surg. 2018;41(3):210–5.

3. Zhang Y. Epidemiology of esophageal cancer. World J Gastroenterol. 2013;19(34):5598–606.

4. Feng RM, Zong YN, Cao SM, Xu RH. Current cancer situation in China: good or bad news from the 2018 global cancer statistics? Cancer Commun. 2019;39(1):22.

5. Ng J, Lee P. The role of radiotherapy in localized esophageal and gastric cancer. Hematol Oncol Clin North Am. 2017;31(3):453–68.

6. Zhou H, Zhang G, Xue X, Yang Y, Yang Y, Chang X, et al. Identification of novel NRAGE involved in the radioresistance of esophageal cancer cells. Tumour Biol. 2016;37(7):8741–52.

7. Kristensen LS, Andersen MS, Stagsted LVW, Ebbesen KK, Hansen TB, Kjems J. The biogenesis, biology and characterization of circular RNAs. Nat Rev Genet. 2019;20(11):675–91.

8. Zhong Y, Du Y, Yang X, Mo Y, Fan C, Xiong F, et al. Circular RNAs function as ceRNAs to regulate and control human cancer progression. Mol Cancer. 2018;17(1):79.

9. Wang HY, Wang YP, Zeng X, Zheng Y, Guo QH, Ji R, et al. Circular RNA is a popular molecule in tumors of the digestive system (review). Int J Oncol. 2020;57(1):21–42.

10. Lei B, Tian Z, Fan W, Ni B. Circular RNA: a novel biomarker and therapeutic target for human cancers. Int J Med Sci. 2019;16(2): 292–301.

11. Yue M, Liu Y, Zuo T, Jiang Y, Pan J, Zhang S, et al. Circ_0006948 contributes to cell growth, migration, invasion and epithelial-mesenchymal transition in esophageal carcinoma. Dig Dis Sci. 2021.

12. Zhang WQ, Liu KQ, Pei YX, Tan J, Ma JB, Zhao J. Circ-ABCB10 promotes proliferation and invasion of esophageal squamous cell carcinoma cells by modulating microRNA-670-3p. Eur Rev Med Pharmacol Sci. 2020;24(11):6088–96.

13. Wang J, Chen Y, Wu R, Lin Y. Circular RNA hsa_circ_0000554 promotes progression and elevates radioresistance through the miR-485-5p/fermitin family members 1 axis in esophageal cancer. Anticancer Drugs. 2021;32:405–16.

14. Su H, Lin F, Deng X, Shen L, Fang Y, Fei Z, et al. Profiling and bioinformatics analyses reveal differential circular RNA expression in radioresistant esophageal cancer cells. J Transl Med. 2016;14(1):225.

15. Lee YS, Dutta A. MicroRNAs in cancer. Annu Rev Pathol. 2009;4: 199–227.

16. Xie C, Wu Y, Fei Z, Fang Y, Xiao S, Su H. MicroRNA-1275 induces radiosensitization in oesophageal cancer by regulating epithelial-to-mesenchymal transition via Wnt/beta-catenin pathway. J Cell Mol Med. 2020;24(1):747–59.

17. Zang C, Zhao F, Hua L, Pu Y. The miR-199a-3p regulates the radioresistance of esophageal cancer cells via targeting the AK4 gene. Cancer Cell Int. 2018;18:186.

18. Park M, Yoon HJ, Kang MC, Kwon J, Lee HW. MiR-338-5p enhances the radiosensitivity of esophageal squamous cell carcinoma by inducing apoptosis through targeting survivin. Sci Rep. 2017;7(1):10932.

19. Zhang YH, Wang QQ, Li H, Ye T, Gao F, Liu YC. miR-124 radiosensitizes human esophageal cancer cell TE-1 by targeting CDK4. Genet Mol Res. 2016;15(2).

20. Xia H, Chen S, Chen K, Huang H, Ma H. MiR-96 promotes proliferation and chemo- or radioresistance by down-regulating RECK in esophageal cancer. Biomed Pharmacother. 2014;68(8):951–8.

21. Zhang Q, Zhang J, Fu Z, Dong L, Tang Y, Xu C, et al. Hypoxia-induced microRNA-10b-3p promotes esophageal squamous cell carcinoma growth and metastasis by targeting TSGA10. Aging. 2019; 11(22):10374–84.

22. Lu YF, Yu JR, Yang Z, Zhu GX, Gao P, Wang H, et al. Promoter hypomethylation mediated upregulation of MicroRNA-10b-3p targets FOXO3 to promote the progression of esophageal squamous cell carcinoma (ESCC). J Exp Clin Cancer Res. 2018;37(1):301.

23. Wang L, Shang X, Feng Q. LncRNA TATDN1 contributes to the cisplatin resistance of non-small cell lung cancer through TATDN1/miR-451/TRIM66 axis. Cancer Biol Ther. 2019;20(3): 261–71.

24. Cui C, Yang J, Li X, Liu D, Fu L, Wang X. Functions and mechanisms of circular RNAs in cancer radiotherapy and chemotherapy resistance. Mol Cancer. 2020;19(1):58.

25. Zhang LW, Wang B, Yang JX, Yang H. Circ-PRMT5 stimulates migration in esophageal cancer by binding miR-203. Eur Rev Med Pharmacol Sci. 2020;24(19):9965–72.

26. Hou Y, Liu H, Pan W. Knockdown of circ_0003340 induces cell apoptosis, inhibits invasion and proliferation through miR-564/TPX2 in esophageal cancer cells. Exp Cell Res. 2020;394(2):112142.

27. Zhang T, Zhou Y, Guan J, Cheng H. Circ_0058058 knockdown inhibits acute myeloid leukemia progression by sponging miR-4319 to regulate EIF5A2 expression. Cancer Biother Radiopharm. 2021.

28. Xue L, Jia T, Zhu Y, Zhao L, Mao J. Down-regulation of circ_0058058 suppresses proliferation, angiogenesis and metastasis in multiple myeloma through miR-338-3p/ATG14 pathway. J Orthop Surg Res. 2021;16(1):723.

29. Handlogten ME, Hong SP, Zhang L, Vander AW, Steinbaum ML, Campbell-Thompson M, et al. Expression of the ammonia transporter proteins Rh B glycoprotein and Rh C glycoprotein in the intestinal tract. Am J Physiol Gastrointest Liver Physiol. 2005;288(5):G1036–47.

30. Chen BS, Xu ZX, Xu X, Cai Y, Han YL, Wang J, et al. RhCG is down-regulated in oesophageal squamous cell carcinomas, but expressed in multiple squamous epithelia. Eur J Cancer. 2002;38(14):1927–36.

31. Ming XY, Zhang X, Cao TT, Zhang LY, Qi JL, Kam NW, et al. RHCG suppresses tumorigenicity and metastasis in esophageal squamous cell carcinoma via inhibiting NF-kappaB signaling and MMP1 expression. Theranostics. 2018;8(1):185–98.

## SUPPORTING INFORMATION

Additional supporting information may be found in the online version of the article at the publisher's website.